Journal of Nano- and Electronic Physics
Vol. **14** No 1, 01028(4pp) (2022)

Журнал нано- та електронної фізики
Том **14** № 1, 01028(4cc) (2022)

Structural, Optical and Electrical Properties of rGO@SnO_2 Nanopowder Obtained via Chemical Co-precipitation Method

Jagat Pal Singh[1,*], G.C. Joshi[2]

[1] *Department of Physics, G.B Pant University of Agri. & Tech., Pantnagar-263145, India*
[2] *RITL, G.B Pant University of Agri. & Tech., Pantnagar-263145, India*

(Received 04 February 2022; revised manuscript received 21 February 2022; published online 28 February 2022)

The chemical co-precipitation technique is used to synthesize rGO@SnO_2 nanopowder. Among a variety of metal oxides, SnO_2 is an *n*-type semiconductor with a broad band gap of 3.64 eV at room temperature, which is widely used in different applications such as sensors, transparent conducting electrodes, optoelectronic devices, photocatalysts, lithium-ion batteries, and solar cells. When analyzing the X-ray diffraction (XRD) spectra, the crystallite size of nanoparticles is 2.15 nm. Fourier transform infrared spectroscopy (FTIR) shows the stretching and vibrational modes of the metal-oxygen bond at 662 cm^{-1}, confirms the presence of antisymmetric O–Sn–O bridge and the appearance of peaks at 1387 cm^{-1} and 1635 cm^{-1} due to C–H and C=C bonds, respectively. Field emission scanning electron microscopy (FESEM) image shows that the size of nanocrystallites is less than 10 nm. The optical band gap (OBG) of rGO@SnO_2 nanopowder is calculated using Tauc plot analysis and is 3.53 eV, which is less than OBG of pure SnO_2. Conductivity and resistivity of rGO@SnO_2 nanopowder are calculated from the *I-V* characteristics.

Keywords: Metal oxide, rGO, FESEM, XRD, Tin oxide, Band gap.

DOI: 10.21272/jnep.14(1).01028 PACS number: 81.07.Wx

1. INTRODUCTION

Nanoscience deals with nanomaterials of nanometer dimensions, and physical and chemical properties of nanoparticles are modified as a result of their creation, which covers a wide range of applications compared to bulk materials. Physical and chemical characteristics have a great impact on the structure of nanoparticles, crystalline nature, and different applications. Metal oxide nanoparticles can be used in various fields, including energy storage, water purification, catalysis, and sensing [1, 2]. Tin oxide (SnO_2) is of interest as a prospective *n*-type semiconductor due to its promising physical and chemical properties. With a wide band gap of 3.6 eV [3] and high thermal stability, nanostructured SnO_2 is widely regarded as a serious contender for the role of photocatalysts and chemical sensors. However, there are several fundamental issues that need to be recognized and solved when considering its practical use. For example, the activity of small size SnO_2 nanoparticles will decrease in the photocatalytic process due to aggregation caused by their high surface energy. Therefore, much attention is paid to the activity of SnO_2/rGO nanocomposites [4]. The high electron-hole recombination rate is detrimental to the photocatalytic efficiency. Application for gas sensing is also limited by the high operating temperature and slow response time associated with the high activation energy of the reaction [5-7]. As a result, much attention has been paid to numerous attempts to improve the performance of nanostructured SnO_2/rGO nanocomposites [8]. Due to the improved electrical characteristics of rGO, SnO_2/rGO nanocomposites are of great interest [9].

In this work, we synthesized rGO@SnO_2 nanopowder via a simple chemical co-precipitation method. Under ambient conditions, rGO@SnO_2 nanomaterials received much attention, and nanoparticles formed on the surface of rGO. This study is very useful for photocatalysts and room temperature gas sensing applications.

2. EXPERIMENTAL

2.1 Materials

All chemicals were used without further purification. Stannic chloride pentahydrate ($SnCl_4.5H_2O$), sodium hydroxide (NaOH), polyethylene glycol 400 (PEG 400) were purchased from Himedia chemicals.

2.2 Method

Reduced graphene oxide (rGO) was synthesized by the modified Hummers method. The prepared suitable volume (1 wt. % $SnCl_4.5H_2O$) of rGO was ultrasonicated for 2 h in 50 ml of deionized water to obtain a homogeneous suspension. A 1 M solution of $SnCl_4.5H_2O$ was stirred for 15 min in 50 ml of double deionized (DDI) water. Then rGO suspension was added to the $SnCl_4.5H_2O$ solution, followed by magnetic stirring of the entire mixture for 15 min. 5 ml of PEG was added to the entire mixture for nanoparticle embolization. The resulting mixture was shaken by a magnetic stirrer at 400 rpm to form a uniform mixture. 1 M aqueous solution of NaOH was added dropwise to the prepared mixture to raise the PH to 12 with continuous stirring. On completion of the reaction, a thick precipitate was found at the bottom of the flask. The whole mixture was stirred for 3 h at 50 °C with a temperature-controlled magnetic stirrer. The precipitate was filtered, and the nanoparticles were washed 4 times with DDI water and twice with ethanol (99 % purity AR grade) to exclude impurities and chloride ions.

The precipitates were extracted from the centrifuge tubes and dried at 70 °C in a hot air oven for 18 h, then

* jagatpalsingh7@gmail.com

collected and ground with a mortar pestle. Eventually, the synthesized powder, placed in a muffle furnace, was calcined at 500 °C for 3 h, and the prepared sample was removed from the crucible.

2.3 Characterization

The obtained nanopowder was collected for characterization. The prepared sample was characterized using XRD, FTIR, and UV-Vis techniques. The structural properties of rGO@SnO_2 nanopowder were studied using X-ray diffractometer measurements; XRD spectra were obtained on a Bruker D8 Advance setup. The Cu-Kα radiation source ($\lambda = 1.5406$ Å) operated at 40 kV at a scan rate of 5°/min over the range of 10-90°. Spectral transmittance and absorbance measurements were performed using a UV-Vis spectrometer (LAMBDA 365, PerkinElmer) in the spectral range of 190 to 1100 nm. The X-intercept obtained to extrapolate the linear part of the exponential curve from the graph of $(\alpha h\nu)^2$ vs photon energy ($h\nu$) represents the band gap energy of the material. Transmittance spectra were recorded using FTIR (Nicolet-6700, Thermo Scientific). Electrical properties were measured using a Keithley SCS-4200 semiconductor characterization system (USA).

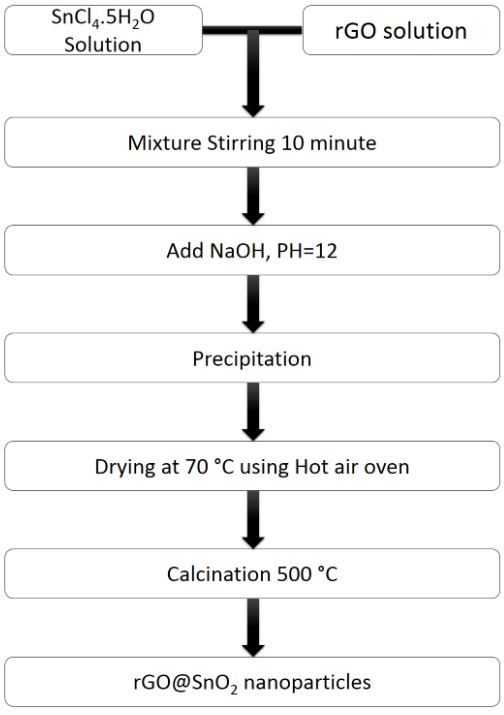

Fig. 1 – Scheme of preparation of rGO@SnO_2 nanopowder

3. RESULTS AND DISCUSSION

3.1 Structural Properties

The XRD patterns of the produced rGO@SnO_2 nanopowders are shown in Fig. 2. The cassiterite structure of SnO_2 is identical to ICDD numbers 41-1445 [10], and the absence of any undesired peaks has shown that no impurities exist. The characteristic peak positions were located at diffraction angles of 26.5, 33.9, 37.95, 38.99, 42.64, 51.78, 54.76, 57.85, 61.77, 65.09, 71.44, 78.62 and 83.95°, corresponding to the (110), (101), (200), (111), (210), (211), (002), (310), (221), (112), (202), (321), and (222) planes, respectively. At the bottom, the peak of the highest intensity plane (101) is visible. The following formulas were used to calculate the crystallite size (D), lattice strain (ε), interplanar distance (d), dislocation density (δ), and the number of crystallites per unit area (N) [11, 12]:

$$D = 0.9\lambda / \beta \cos\theta, \quad (1)$$

$$\varepsilon = \beta \cos\theta / 4, \quad (2)$$

$$d = \lambda / 2\sin\theta, \quad (3)$$

$$\delta = 1 / D^2, \quad (4)$$

$$N = d / D^3, \quad (5)$$

where θ is the diffraction angle, β is the FWHM (full width at half maximum) of the peak (101), and λ is the wavelength of radiation used (1.54 Å).

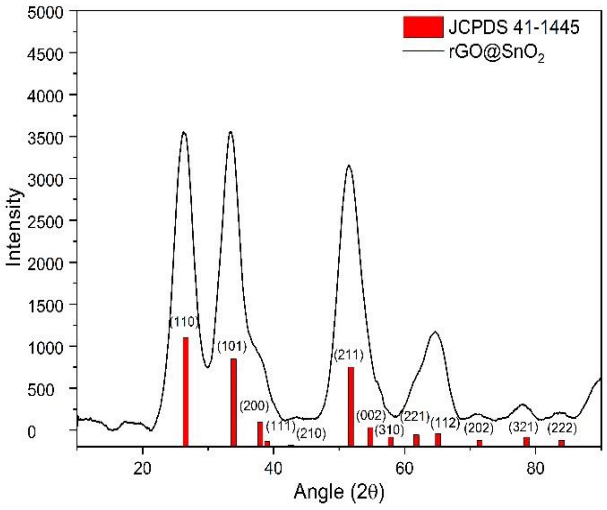

Fig. 2 – X-ray diffraction pattern of rGO@SnO_2 nanopowder

3.1 Morphological Properties

Morphology of the synthesized nanoparticles was determined by FESEM analysis. FESEM micrographs clearly indicate the formation of nanoparticles of controlled size and regular shape. Carbon may surround Sn particles or be located between them, resulting in a reduction of particle size and minimization of particle agglomeration.

3.2 FTIR Analysis

The number of absorption peaks and the position of the bands depend on the chemical composition, morphology and crystalline structure [13]. Predicting the presence of certain functional groups is quite useful in the transmission mode of the FTIR technique, which are adsorbed at different frequencies, hence revealing the structure of the material. The surface of sintered samples in the wave number range 400-4000 cm^{-1} was analyzed by FTIR to investigate chemical clusters at

Table 1 – Parameters calculated by XRD analysis

Sample	Plane	Angle 2θ (degree)	FWHM β (degree)	Crystallite size D (nm)	Lattice strain $\varepsilon \times 10^{-5}$	Interplanar distance d (Å)	Dislocation density δ (m^{-2})×10^{14}	Number of crystallites per unit area N (m^{-2})×10^{12}
rGO@SnO_2	(101)	33.5	4.02	2.15	0.0167	2.27	0.215	0.227

room temperature. A strong peak extending from 3500 to 2500 cm^{-1} indicates the involvement of hydrogen bonds in the O–H oscillators, which may be due to the Sn–OH group formed upon absorption of water. The presence of rGO in the sample is confirmed by the C–H and C=C modes corresponding to the peaks at 1387 cm^{-1} and 1635 cm^{-1}, respectively. The absorption of CO_2 is confirmed by a weak absorption peak visible at 2117 cm^{-1} in ambient atmosphere [14]. The peaks appearing at 585 cm^{-1} and 662 cm^{-1} due to the Sn–O stretching mode of vibration and antisymmetric Sn–O–Sn mode of vibration for the sample under study are shown in Fig. 4.

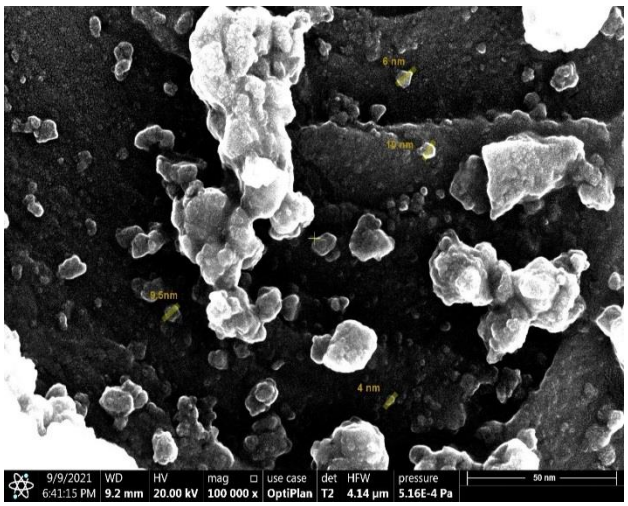

Fig. 3 – Surface morphology by FESEM analysis of rGO@SnO_2 nanopowder

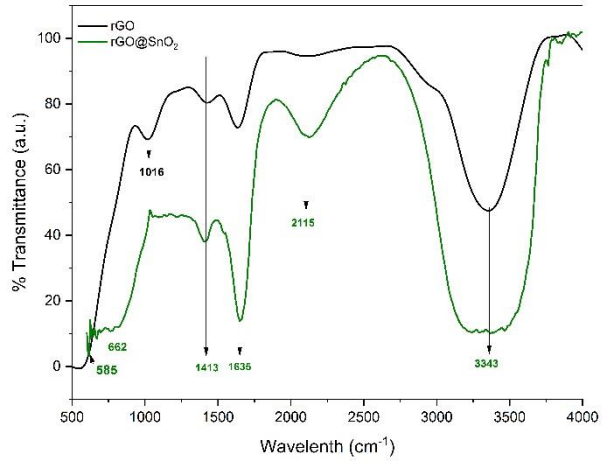

Fig. 4 – FTIR spectra of rGO@SnO_2 nanopowder

3.3 Optical Properties

One of the most used and non-destructive methods for estimating the optical characteristics of synthesized samples is the optical absorption technique. The UV-Visible spectra of rGO@SnO_2 nanopowder are shown in Fig. 5. The absorption peak in this region if found to be between 250 and 350 nm. The creation of shallow levels can be due to doping, which causes the formation of absorption bands inside the band gap. The growth and accumulation of radiation-induced defects that act as color centers may explain the decrease in absorbance of the studied samples. The band gap of materials can be estimated using the absorption coefficient (a) and photon energy (hv):

$$\alpha h\nu = A\left(h\nu - E_g\right)^n, \tag{6}$$

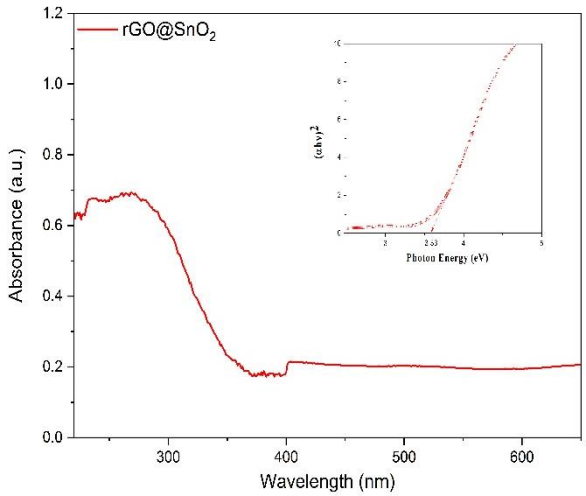

Fig. 5 – UV-Vis absorbance spectra of rGO@SnO_2

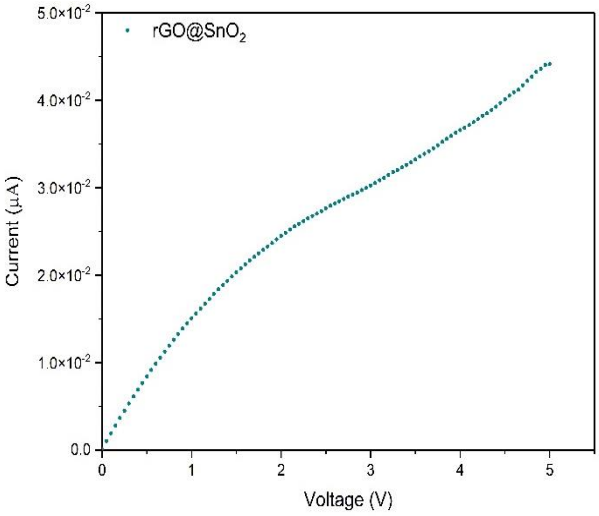

Fig. 6 – *I-V* characteristic of rGO@SnO_2

where A is a constant, α is the absorption coefficient, OBG of the material is denoted by E_g, and n is the number of allowed direct and indirect transitions. Because of the allowed direct transition, n is set to 1/2 in this scenario.

Table 2 – Conductivity and resistivity of rGO@SnO_2 at + 5 V

Samples	Resistivity (Ω·cm)	Conductivity $(\Omega\cdot cm)^{-1}$	OBG (eV)
rGO@SnO_2	5.67×10^{6}	1.76×10^{-7}	3.53

The graph is extrapolated to the $h\nu$ axis to calculate the value of OBG for the samples. With increasing dose of gamma radiation, the band gap of rGO@SnO_2 nanopowder is 3.53 eV, as shown in Fig. 5. The obtained OBG of rGO@SnO_2 is less than the OBG of bulk SnO_2 which is 3.6 eV. This change may be due to rGO as well as the quantum confinement effect.

3.4 Electrical Properties

Fig. 6 shows the *I-V* characteristic of rGO@SnO_2. It is seen from the graph that as the voltage increases to + 5 V, the current value increases. Table 2 lists the values of conductivity and resistivity.

4. CONCLUSIONS

In this research work, rGO@SnO_2 nanopowder was synthesized by chemical co-precipitation technique. The crystallite size of synthesized nanoparticles obtained by XRD analysis turned out to be 2.15 nm. The FESEM image showed that the particles size is in the range of 4-10 nm without any specific structure. The OBG value of 3.53 eV was obtained by analyzing the Tauc plot. The conductivity of the samples of 1.76×10^{-7} $(\Omega.cm)^{-1}$ was calculated from the *I-V* characteristics. In the future, this research work could be very useful for photocatalysts and room temperature gas sensing applications.

ACKNOWLEDGEMENTS

The authors are thankful to the Laboratory of Biophysics (G.B. Pant University of Agriculture and Technology, Pantnagar, India) for providing laboratory facility for this research work.

REFERENCES

1. Z. Ying, Q. Wan, Z.T. Song, S.L. Feng, *Nanotechnology* **15** No 11, 1682 (2004).
2. A.K. Singh, U.T. Nakate, *Adv. Nanoparticles* **2** No 1, 66 (2013).
3. K.P. Gattu, K. Ghule, A.A. Kashale, V.B. Patil, D.M. Phase, R.S. Mane, S.H. Han, R. Sharma, A.V. Ghule, *RSC Adv.* **5** No 89, 72849 (2015).
4. A. Ahmed, M.N. Siddique, U. Alam, T. Ali, P. Tripathi, *Appl. Surf. Sci.* **463**, 976 (2019).
5. M. Mathew, P.V. Shinde, R. Samal, C.S. Rout, *J. Mater. Sci.* **56** No 16, 9575 (2021).
6. A. Krishnakumar, P. Srinivasan, A.J. Kulandaisamy, K.J. Babu, J.B.B. Rayappan, *J. Mater. Sci. Mater.* **30** No 18, 17094 (2019).
7. Y.F. Sun, S.B. Liu, F.L. Meng, J.Y. Liu, Z. Jin, L.T. Kong, J.H. Liu, *Sensors* **12** No 3, 2610 (2012).
8. X. Liu, S. Cheng, H. Liu, S. Hu, D. Zhang, H. Ning, *Sensors* **12** No 7, 9635 (2012).
9. F. Meng, H. Zheng, Y. Chang, Y. Zhao, M. Li, C. Wang, J. Liu, *IEEE Trans Nanotechnol.* **17** No 2, 212 (2018).
10. R.A. Nachiar, S. Muthukumaran, *Opt. Laser Technol.* **112**, 458 (2019).
11. H.U. Lee, K. Ahn, S.J. Lee, J.P. Kim, H.G. Kim, S.Y. Jeong, C.R. Cho, *Appl. Phys. Lett.* **98** No 19, 193114 (2011).
12. M.R. Waikar, A.A. Shaikh, R.G. Sonkawade, *Vacuum* **161**, 168 (2019).
13. M. Ashokkumar, S. Muthukumaran, *Opt. Mater.* **37** C, 671 (2014).
14. Y. Yuan, Q. Jiang, J. Yang, L. Feng, *J. Mater. Sci. Mater.* **27** No 9, 9541 (2016).

Структурні, оптичні та електричні властивості нанопорошку rGO@SnO_2, отриманого методом хімічного співосадження

Jagat Pal Singh[1], G.C. Joshi[2]

[1] *Department of Physics, G.B Pant University of Agri. & Tech., Pantnagar-263145, India*
[2] *RITL, G.B Pant University of Agri. & Tech., Pantnagar-263145, India*

Для синтезу нанопорошку rGO@SnO_2 використовується техніка хімічного співосадження. Серед різноманітних оксидів металів SnO_2 є напівпровідником *n*-типу з широкою забороненою зоною 3,64 еВ при кімнатній температурі, який широко використовується в різних додатках, таких як датчики, прозорі провідні електроди, оптоелектронні пристрої, фотокаталізатори, літій-іонні батареї та сонячні елементи. При аналізі спектрів рентгенівської дифракції (XRD) розмір кристалітів наночастинок становить 2,15 нм. Інфрачервона спектроскопія з перетворенням Фур'є (FTIR) показує розтяжні та коливальні режими зв'язку метал-кисень при 662 $см^{-1}$, підтверджує наявність антисиметричного містка O–Sn–O і появу піків при 1387 $см^{-1}$ та 1635 $см^{-1}$ за рахунок зв'язків C–H та C=C відповідно. Зображення автоелектронної скануючої мікроскопії (FESEM) показує, що розмір нанокристалітів менше 10 нм. Оптична ширина забороненої зони (OBG) нанопорошку rGO@SnO_2, розрахована за допомогою аналізу графіка Тауца, становить 3,53 еВ, що менше, ніж OBG чистого SnO_2. Провідність та питомий опір нанопорошку rGO@SnO_2 розраховано за вольт-амперними характеристиками.

Ключові слова: Оксид металу, rGO, FESEM, XRD, Оксид олова, Заборонена зона.